Nonlinear Modelling, Dynamic Performances and control of an Electrical Syringe Pump Using a Linear Actuator

IMED MAHMOUD[1,3], [2,3]ADEL KHEDHER
[1]Department of Electrical Engineering, Higher Institute of Applied Science and Technology Mahdia, TUNISIA
[2]Department of Electrical Engineering, National Engineering School of Sousse, TUNISIA
[3]Laboratory of Advanced Technology and Intelligent Systems (LATIS), TUNISIA

Abstract: - This article discusses the non-linear improved modelling approach, dynamic performances with and without saturation and closed loop control of an electrical syringe pump using a linear actuator. This work is intended for the mathematical characterization and setting equation of LSRM including the effect of magnetic nonlinearities. The work is beginning by the modelling of the inductance variation versus current. This variation is analytically described using Fourier series and the polynomial functions are used to express the nonlinear variation of its coefficients versus current. The second step is reserved to the prediction of the dynamic performances, taking into account the saturation phenomenon. Finally, the linear stepper motors movement is characterized by a highly oscillatory translation, which is troublesome for the positional accuracy and the speed constant such as depend by many industrial applications such as the syringe pump. Thus, in order to attenuate the amplitudes of these oscillations and guarantee the positioning of the actuator without errors, solutions exploiting closed-loop control techniques are proposed in this paper for the purpose of improve the actuator performances.

Key-Words: - linear motor, electrical syringe pump, nonlinear inductance, Fourier series, FEM, saturation.
Received: October 14, 2022. Revised: April 24, 2023. Accepted: June 5, 2023. Published: July 7, 2023.

1 Introduction

The syringe pump is a conventional biomedical system hospital emergency service. It is mainly used in intravenous, intra-arterial infusions, anesthetic infusions and chemotherapy. It is essential in the various general surgery departments and the internal department of medicine for children, adults, pediatrics, the emergency department, gynecology, and soon.

Perfusion is a continuous drug delivery method over time at a constant rate. Whatever the nature of the disease, the infusion treatment is all the more effective that the injected doses are balanced and regularly distributed over time.

The satisfaction of this requirement needs the use of syringe pumps whose technology is constantly evolving in search for performance improvement, [1-2]. Motorization of this electrical syringe pump is often ensured by a Linear Stepping Motor.

Nowadays, LSRM are widely used. Unfortunately, in order to generate a high-propulsion force the LSRM must be operated in the saturation zone. In saturation conditions, main magnetic characteristics, such as flux linkage, inductance and propulsion force, are highly nonlinear. Modeling and simulation of a switched reluctance machines is more complex than that of AC and DC motors due to its highly non-linear operation. These nonlinearities are introduced by two main factors: Magnetic saturation and the air gap variation. Consequently, the model based on some hypotheses are not very accurate to determine system performances and elaborate control strategies, [3- 4].

The LSRM is always operating in the magnetically saturated mode to maximize the energy transfer. In a LSRM, the phase inductances and flux linkages vary with rotor position due to stator and rotor saliencies. The phase inductances and flux linkages at any rotor position also vary with the instantaneous phase currents because of magnetic saturation. However, these variations can be modelled analytically using the obtained data through FEM or via experiments. These analytical expressions are used to represent the LSRM dynamics and hence the machine performances can be obtained, [5-6-7-8-9-10].

There has been widespread research in the Linear Switched Reluctance Motor modelling area, which includes the effect of magnetic nonlinearities. However, there is still a lack of accuracy. For this purpose, this paper provides an improvement of the classical approach formerly known, [11-12-13-14-21].

The paper is organized as follows. Taking apart the introduction and the conclusion, section 1 gives the dimensional characteristics of the used motor and syringe. Section 2 details the proposed improved model and compares to the results extracted from the FEM. Section 3 is reserved to determine the dynamic performances including the magnetic nonlinearities effect. Finally, Section 4 is to suggest closed loop control approaches taking into account the dynamic behavior ensuring precise positioning and without overshoot for different medication infusion rates.

2. Dimensional characteristics of the all biomedical system.

The stepping linear motor, thanks to its reliability and control simplicity, is used in various applications such as robotics, machine tools ordering, space applications and military and data-processing peripherals. In the medical field, it is largely used as well for the displacement and the shunting of the surgical laser beams as for medical scanners piloting apparatuses. The Descriptive diagram of the all biomedical system, to be studied, is illustrated by Figure 1 where all geometrical parameters are defined.

Some mechanical and electrical parameters of the actuator and syringe are given in table 1 **(appendix).**

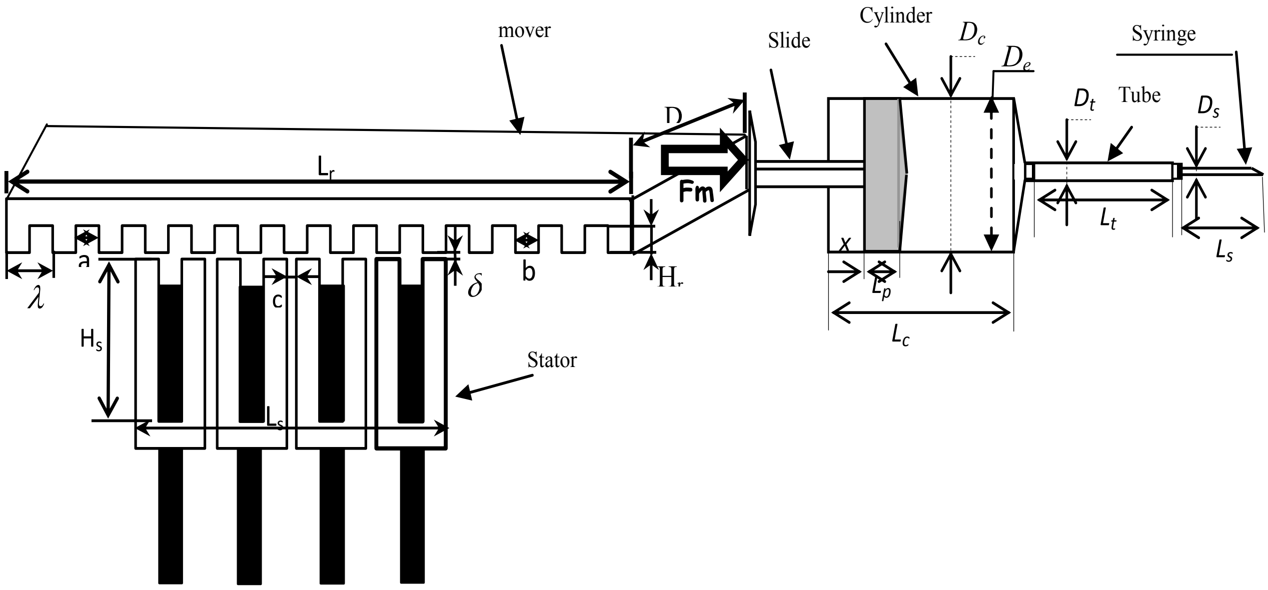

Fig.1. *Block diagram representation of the biomedical system*

Figure 1. Block diagram representation of the biomedical system

3. Analytical model of the LSRM

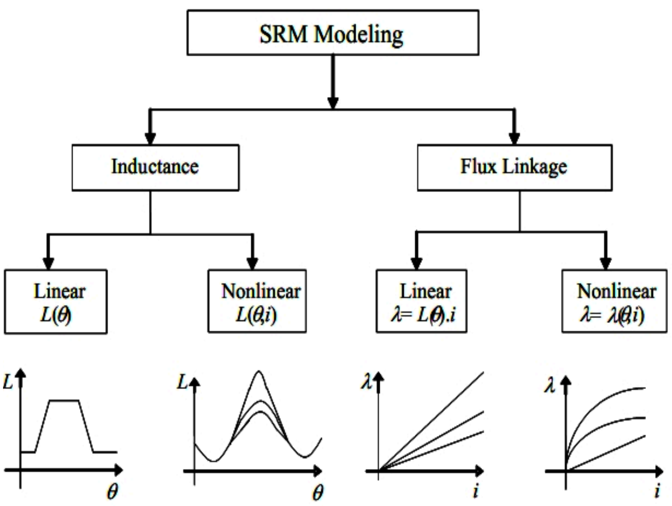

Figure 2. Classification of LSRM modelling

In order to determine the non-linear improvement modelling approach which describes the behavior of a saturated reluctant structure, there are basically two ways to represent the static LSRM characteristics. The first is to plot the phase flux linkage variations with rotor position and phase current. The second one is to plot the phase inductance variation with rotor position at different phase currents. These static characteristics are highly nonlinear. Figure 2 shows a classification of the different LSRM modelling techniques.

In LSRM, the magnetic reluctance is strongly affected by the nonlinear characteristic of the employed magnetic matters. Consequently, this variation is reflected on the inductance evolution. Accordingly, the phase inductance changes periodically as function of the rotor position. At any given rotor position, the phase inductance also varies with the instantaneous phase current as shown in the figure 3. It is maximum in the aligned position and minimum in the unaligned position.

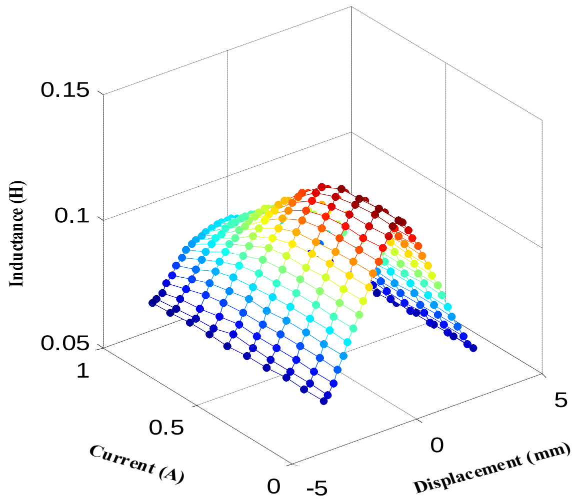

Figure 3. Response surface of the inductance as a function of position and current.

Therefore, the phase inductance versus mover position will be represented by Fourier series (1) and the nonlinear variation of its coefficients with current will be expressed by polynomial functions (6, 7 and 8), [16-18-23-24-26]:

$$L(x,i)=\sum_{k=0}^{m} L_k(i)\cos kN_r x \qquad (1)$$

With $i, x \, and \, m$ are respectively the phase current, the mover position and the number of Fourier series terms.

The numerical simulations accuracy and stability are the main challenges which should be met. To simplify Eq (1), by considering the first three terms of the Fourier series are considered. The inductance expression is given by Eq (2), [15-17-20-21]:

$$L(x,i_j)=L_0(i_j)+L_1(i_j)\cos\left(N_r\left(x-(j-1)\frac{2\pi}{NN_r}\right)\right) + L_2(i_j)\cos\left(2N_r\left(x-(j-1)\frac{2\pi}{NN_r}\right)\right) \qquad 2)$$

With $L(x,i_j)$ is the inductance associate to the phase j in the mover position x for the current i_j and N the phase number.

The analytical model can be developed by employing a curves number depending on the Fourier series order. A second order Fourier series requires three positions to determine three coefficients L_0, L_1 and L_2. The useful operation of the actuator extends from the starting position x = 1.5 mm to the position of conjunction x = 0 mm. It follows that the description of the indispensable intermediate position, such that x = 0.75mm.

To determine the three coefficients $L_0, L_1 \, and \, L_2$, we use the inductance at three positions: $L(x=0\,mm)$, $L(x=0.75\,mm)$ and $L(x=1.5\,mm)$.

Therefore, these three coefficients are written as follows:

$$L_0=\frac{1}{\sqrt{2}-1}\left[\frac{\sqrt{2}}{2}(L(0)+L(1.5))-L(0.75)\right] \qquad (3)$$

$$L_1=\frac{1}{\sqrt{2}-1}\left[-L(0)-L(1.5)+2L(0.75)\right] \qquad (4)$$

$$L_2=\frac{1}{\sqrt{2}-1}\left[\frac{\sqrt{2}}{2}L(0)+\left(1-\frac{\sqrt{2}}{2}\right)L(1.5)-L(0.75)\right] \qquad (5)$$

The inductance $L(i)_{x=0\,mm}$, $L(i)_{x=0.75\,mm}$ and $L(i)_{x=1.5\,mm}$ are function of the phase current and can be approximated by polynomials as follows:

$$L_{ij}(x=0)=\sum_{n=0}^{p} a_n i^n{}_j \qquad (6)$$

$$L_{ij}(x=0.75)=\sum_{n=0}^{p} b_n i^n{}_j \qquad (7)$$

$$L_{ij}(x=1.5)=\sum_{n=0}^{p} c_n i^n{}_j \qquad (8)$$

With p is the order of the polynomials and a_n, b_n, c_n their coefficients. In our study, p=6 was considered sufficient for an adequate description, Figure 4.

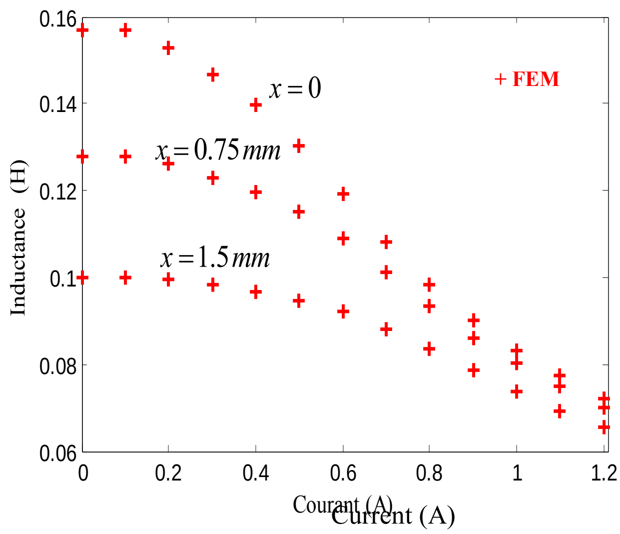

Figure 4. Inductance against phase current for three positions.

The inductance curve versus current in position $x=0mm$ was approximated using the following polynomial:

$$L(i)_{x=0mm}=a_6 i^6+a_5 i^5+a_4 i^4+a_3 i^3+a_2 i^2+a_1 i+a_0 \qquad (9)$$

In a similar way, we find:

$$L(i)_{x=0.75mm}=b_6 i^6+b_5 i^5+b_4 i^4+b_3 i^3+b_2 i^2+b_1 i+b_0 \qquad (10)$$

$$L(i)_{x=1.5mm}=c_6 i^6+c_5 i^5+c_4 i^4+c_3 i^3+c_2 i^2+c_1 i+c_0 \qquad (11)$$

The polynomial description of functions $L(i)_{x=0\,mm}$, $L(i)_{x=0.75\,mm}$ and $L(i)_{x=1.5\,mm}$ in Eqs (9), (10) and (11) gives the functions $L_0(i), L_1(i)$ and $L_2(i)$ described in Eqs (3), (4) and (5) so that:

$$L_0(i) = d_6 i^6 + d_5 i^5 + d_4 i^4 + d_3 i^3 + d_2 i^2 + d_1 i + d_0 \qquad (12)$$

$$L_1(i) = e_6 i^6 + e_5 i^5 + e_4 i^4 + e_3 i^3 + e_2 i^2 + e_1 i + e_0 \qquad (13)$$

$$L_2(i) = h_6 i^6 + h_5 i^5 + h_4 i^4 + h_3 i^3 + h_2 i^2 + h_1 i + h_0 \qquad (14)$$

All coefficients of Eqs (9), (10), (11), (12), (13) and (14) are given in Tables 2 **(Appendix).**

Figure 5 shows the comparison between the inductance characteristics obtained by the improvement proposed model and the obtained result through FEM.

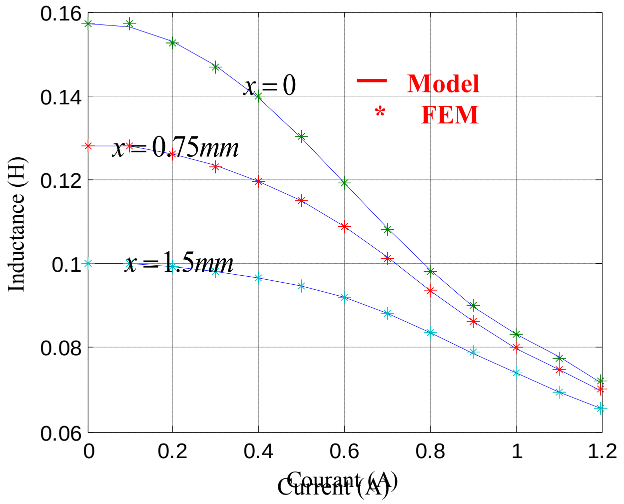

Figure 5. Comparison of the inductance characteristics against phase current for three positions.

In addition, it is to be noted that by multiplying the expression of the inductance by the current one derives that of the flux.

$$\varphi(i)_x = L(i)_x\, i \qquad (15)$$

The stator phase inductance at the aligned position is very affected by the stator phase current variations. On the contrary, the unaligned inductance is practically constant due to the large reluctance that characterizes this position.

It is worth mentioning that, the found analytical model remains valid for any position **"x"** and any current **"i"** as illustrated by figures 5 and 6. These figures provide better characteristics predetermination.

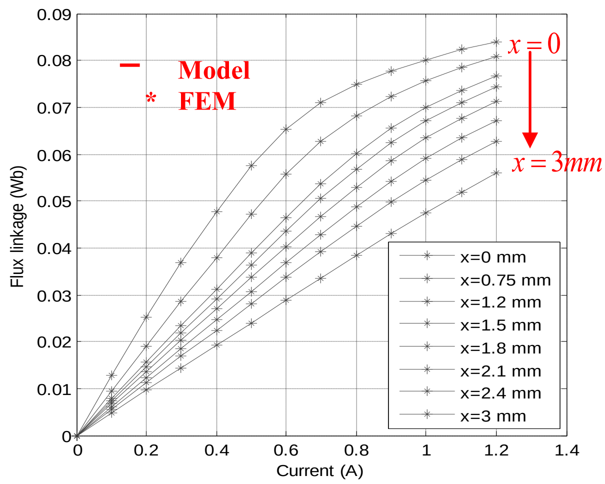

Figure 6. Flux characteristics Versus current for different positions.

4. Dynamic behaviour of the biomedical application

The actuator is coupled with the syringe plunger in presence of the aqueous solution to perfuse. We plan to study the dynamic behavior of all biomedical application. It is well known that the total electromagnetic force is given by the following expression, [19-22-25-26]:

$$F_j(i,x) = \frac{\partial W_{c,j}}{\partial x} = \frac{\partial \left(\int_0^i L(x, i_j)\, i_j\, di_j \right)}{\partial x} \qquad (16)$$

For a given current, equation (16) becomes:

$$F_j(i,x) = \frac{1}{2} \frac{\partial L_j(x)}{\partial x} i_j^{\,2} \Big|_{[i]=cte} \qquad (17)$$

After development we get:

$$F(i,x) = -\frac{2\pi}{\lambda}\sin\left(\frac{2\pi}{\lambda}x\right)\int_0^i L_1(i)\, i\, di - \frac{4\pi}{\lambda}\sin\left(\frac{4\pi}{\lambda}x\right)\int_0^i L_2(i)\, i\, di$$

(18)

With:

$$\int_0^i L_1(i)\, i\, di = \sum_{k=2}^{8} \frac{1}{k}\, e_{k-2}\, i^k \qquad (19)$$

$$\int_0^i L_2(i)\, i\, di = \sum_{k=2}^{8} \frac{1}{k}\, h_{k-2}\, i^k \qquad (20)$$

Remember that the coefficients e_k and h_k are defined previously. Finally the total electromagnetic force is given by:

$$F(i,x) = -\left[\sum_{k=2}^{8} \frac{1}{k}\, e_{k-2}\, i^k\right] \frac{2\pi}{\lambda} \sin(\frac{2\pi}{\lambda} x) - \left[\sum_{k=2}^{8} \frac{1}{k}\, h_{k-2}\, i^k\right] \frac{4\pi}{\lambda} \sin(\frac{4\pi}{\lambda} x) \quad 21)$$

The four phases of LSRM are described by these dynamic electric equations as follows:

$$U_A = Ri_A + L(x,i_A)\frac{di_A}{dt} + i_A\left(\frac{\partial L(x,i_A)}{\partial x}\frac{dx}{dt} + \frac{\partial L(x,i_A)}{\partial i_A}\frac{di_A}{dt}\right)$$
(22)

$$U_B = Ri_B + L(x,i_B)\frac{di_B}{dt} + i_B\left(\frac{\partial L(x,i_B)}{\partial x}\frac{dx}{dt} + \frac{\partial L(x,i_B)}{\partial i_B}\frac{di_B}{dt}\right)$$
(23)

$$U_C = Ri_C + L(x,i_C)\frac{di_C}{dt} + i_C\left(\frac{\partial L(x,i_C)}{\partial x}\frac{dx}{dt} + \frac{\partial L(x,i_C)}{\partial i_C}\frac{di_C}{dt}\right)$$
(24)

$$U_D = Ri_D + L(x,i_D)\frac{di_D}{dt} + i_D\left(\frac{\partial L(x,i_D)}{\partial x}\frac{dx}{dt} + \frac{\partial L(x,i_D)}{\partial i_D}\frac{di_D}{dt}\right)$$
(25)

For the given phases the derivative of the inductances is given by:

$$\frac{\partial L(x,i)}{\partial x} = -\frac{2\pi}{\lambda} L_1(i)\sin(\frac{2\pi}{\lambda}x) - \frac{4\pi}{\lambda} L_2(i)\sin(\frac{4\pi}{\lambda}x) \quad (26)$$

$$\frac{\partial L(x,i)}{\partial i} = L_0'(i) + L_1'(i)\cos(\frac{2\pi}{\lambda}x) + L_2'(i)\cos(\frac{4\pi}{\lambda}x) \quad (27)$$

With:

$$L_0'(i) = \sum_{k=1}^{6} k\, d_k\, i^{k-1} \quad (28)$$

$$L_1'(i) = \sum_{k=1}^{6} k\, e_k\, i^{k-1} \quad (29)$$

$$L_2'(i) = \sum_{k=1}^{6} k\, h_k\, i^{k-1} \quad (30)$$

$L_0'(i)$, $L_1'(i)$ and $L_2'(i)$ represent the derivative of Eq (12) (13) and (14).

The mechanical equation relating the rotor acceleration, speed, position and load force is by Eq (31).

$$m_c \frac{dx^2}{dt^2} = F(x) - \xi\frac{dx}{dt} - F_0 signe\left(\frac{dx}{dt}\right) - F_r \quad (31)$$

Parameters m_c, ξ, F_0 and F_r mean respectively the actuator mass, the viscous friction force, the dry friction force and the load force. The syringe force F_r is given by this equation.

$$F_r = m_s\frac{d^2x}{dt^2} + C_1 x\frac{dx}{dt} + C_2\left(\frac{dx}{dt}\right)^2 + C_3\frac{dx}{dt} = F_a \quad (32)$$

With: $C_1 = \eta - 8\pi\rho\nu$, $C_2 = \pi\,(\frac{K_1}{D_t^2} + \frac{K_2}{D_s^2} + \frac{K_3}{D_v^2})\,\rho\, D_c^4/8$, $C_3 = 8\rho\,\nu\,(L_d + L_t\frac{D_c^2}{D_t^4} + L_s\frac{D_c^2}{D_s^4})D_c^2$, $L_d = L_c - L_p$, $\eta = \rho\nu\pi D_c$ and $F_a = F_m - \frac{\pi D_c^2 P_p}{4}$

Parameters ν, ρ, P_p and η designate the kinematic viscosity, the density, the blood pressure and the dynamic viscosity.

In order to validate the proposed accuracy model, Malab/Simulink was used to perform the simulation with this model. This last, has been tested and compared by the linear model to predict the dynamic performance of the LSRM.

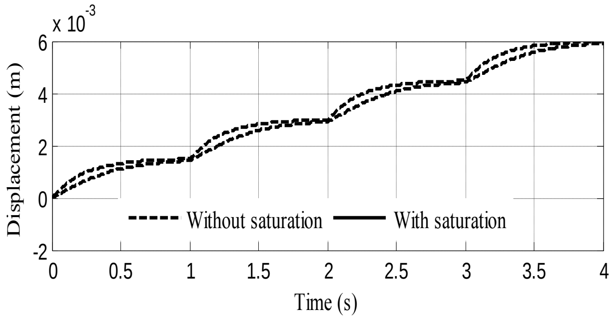

a- Displacement

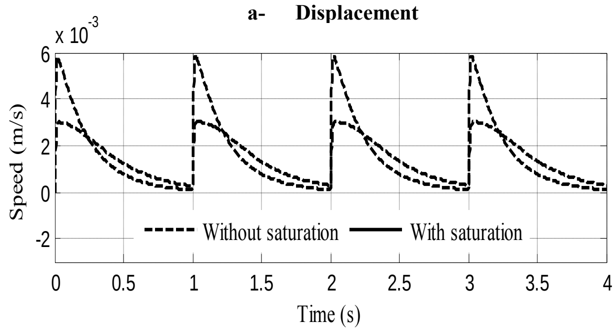

b- Speed

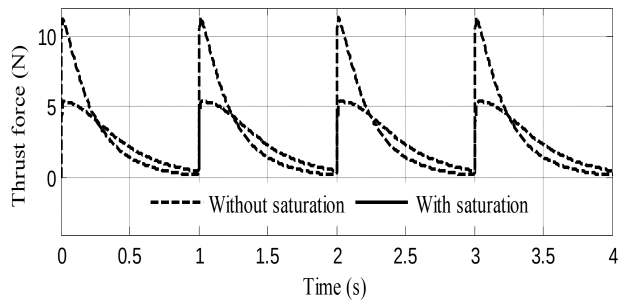

c- Thrust force

Figure 7. Dynamic performances for the biomedical system (actuator-syringe)

Dynamic behavior of displacement thrust force and speed are resumed in figure 7. Note that, the phase A excitation allows positioning of the translator on the first step corresponding to 1.5 mm. Successive excitation of other phases are needed for next steps.

Although it works in open loop, the system is characterized by lack of oscillations. The rotor movement is almost linear and there is practically no need for a closed loop control. The saturated model is characterized by a strongly oscillatory speed and thrust force compared to the linear one. These oscillations are expected to disturb the position accuracy and the speed constancy is often required by many industrial applications and especially in the medical fields. This problem often leads to synchronism losses.

5. closed-loop control of the linear stepper motor

To synthesize the transfer function, it is considered that the machine operates at a vacuum $F_r = 0$ and the mobile movement is ahead where $sign(V) > 0$ and $F_0 = 0$. Equation (31) becomes:

$$m_c \frac{dx^2}{dt^2} = F(i,x) - \xi \frac{dx}{dt} \quad (33)$$

The transfer function between the position **x** and the thrust force **F** is given by equation (35).

$$m_c s^2 x(s) + \xi s x(s) = F(s) \quad (34)$$

$$G(s) = \frac{x(s)}{F(s)} = \frac{1}{m_c s^2 + \xi s} \quad (35)$$

Moreover, the one phase thrust force is expressed by:

$$F(i,x) = -ki^2 \sin(\frac{2\pi}{\lambda} x) \quad (36)$$

Where $k = \frac{\pi L_1}{\lambda}$.

But for each movement sequence, the actuator is incremented by a step given by Eq (37):

$$x = \frac{\lambda}{4} + \Delta x \quad (37)$$

Whether:

$$\sin(\frac{2\pi}{\lambda} x) = \sin(\frac{2\pi}{\lambda}(\frac{\lambda}{4} + \Delta x)) = \sin(\frac{\pi}{2} + \frac{2\pi}{\lambda}\Delta x) = \cos(\frac{2\pi}{\lambda}\Delta x) \quad (38)$$

Since Δx is weak then $\cos(\frac{2\pi}{\lambda}\Delta x) \simeq 1$

From where:

$$F(i,x) = -ki^2 \quad (39)$$

Following these developments, the block diagram of the closed loop control of the motor can be established by Figure.8.

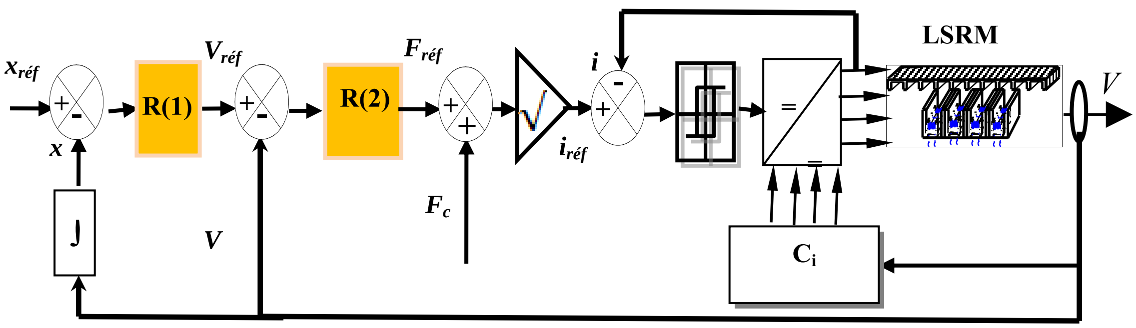

Figure 8. Closed loop control of the motor

This control configuration requires two regulators. A proportional regulator R(1) of gain k_{p1} for evaluating the reference speed V_{ref} and a proportional integral regulator R(2) gains k_{p2} and integral action T_i which serves to determine the reference force F_{ref}. According to the expression (39), the reference current i_{ref} can be used to control the converter. The load force F_c developed by the syringe is added to the system as a disturbance. Regulator gains are determined by the pole compensation method.

Simulation results for a time of the order of unity infusion, figure.9 illustrates the dynamic behavior of the assembly from control current, position, speed and thrust force on a whole step.

In the case of a linear reference, the rotor movement is also perfectly linear. It can be observed that the control law functions correctly with a trajectory tracking with a very high precision, figure.9 (a). As expected, the current is chopped to satisfy the motion linearity, Figure.9 (b). The average speed remains constant around 1.510^{-3}m/s, figure.9 (c). As for the Thrust force, it remains positive average value canceling at the end of the step which is consistent with the operation principle, Figure.9 (d). On the other hand, the phase A excitation allows the positioning of the actuator on the first equilibrium position corresponding to 1.5 millimeters. The successive excitation of the other phases is necessary for the next positions.

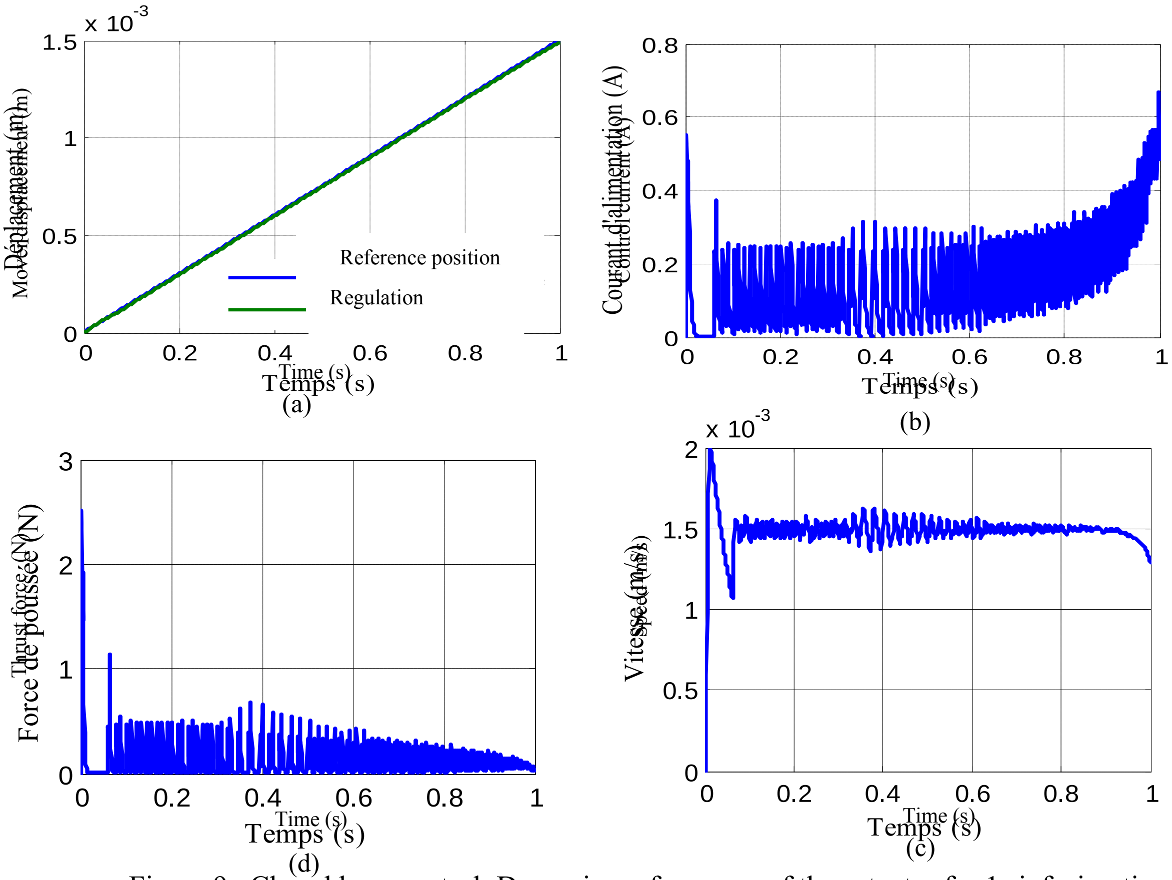

Figure 9. Closed loop control: Dynamic performance of the actuator for 1s infusion time
(a) : Mover displacement (b) : Control current (c) : Speed (d) : Thrust force

The closed-loop control has therefore brought undeniable improvements to the linear stepper movement and the control strategy has led to satisfactory results.

The dynamic performances of the all biomedical system during an infusion depend on the interaction of several parameters characterizing the volume of infusion $V_{infusion}$, the syringe geometry ($L_c = 118mm$ and $V_c = 60ml$) and the Tooth pitch of the actuator $\lambda = 6mm$. These parameters are related by the following expression:

$$V_{infusion} = \frac{\lambda}{L_c} V_c \tag{40}$$

Table 3 **(appendix)** shows that the infusion time is proportional to the volume of aqueous solution to be infused. For instance, an infusion volume of 1.5 ml of sodium chloride corresponds to an infusion time of four seconds which requires one power cycle of the actuator. According to the nature of the disease and the patient, the infusion volume is increased or decreased and consequently the infusion time. In this case, it is necessary to repeat or split the power cycle of the actuator according to the need.

6. Conclusion

The magnetic materials have nonlinear properties which are mainly illustrated by the hysteresis phenomena and saturation. For this purpose, this paper focuses on the modelling, dynamic characteristics and closed loop control of a biomedical system. To predict the motor electromagnetic characteristics, an analytical model of the LSRM is presented taking into account the magnetic circuit nonlinearity. Results are compared to those obtained via the 2D-FEM. The comparison shows a reasonable agreement, proving the validity of the proposed approaches. Then, dynamic performances with and without saturation for the all biomedical system are presented and discussed. Finally, in order to solve the movement problem regularity, an essential factor characterizing the medical application. To overcome the limitations and inadequacies of conventional control techniques, a control concept based on closed-loop control is developed. The application of this control strategy made it possible to enslave the system and force it to follow rigorously the linear reference without overshoots and oscillations.

In the perspective of this work, our contribution will be paid to the implementation of an Experimental bench of the biomedical system for a real validation.

References

[1]. M. N. Lakhoua and S. Laifi. (2011). Overview of quality assurance methods for analysis and modeling of medical processes, International Transactions on Systems Science and Applications, Vol. 7, No. 3/4, pp. 192-203.

[2]. R. Assan, G. Reach and P. Poussier. (1981). Control glycemia and insulin treatment in surgical medium, Technicals manuals, 728-729.

[3]. K Ahmed. (2007). A Fourier Series Generalized Geometry-Based Analytical Model of Switched Reluctance Machines, IEEE transactions on industry application) An Improved Force Distribution Function for Linear Switched Reluctance Motor on Force Ripple Minimization With Nonlinear Inductance Modeling, IEEE Transactions on Magnetics, vol.48, no.11, pp.3064-3067.

[6]. L.Li, M. Mingna, Y.Tang, Z.He, and Q. Chen. (2012). Iron Loss and Inductance Analysis Considering Magnetic Nonlinearity in Multi-Segmented Plate Permanent Magnet Linear Motor, IEEE TRANSACTIONS ON MAGNETICS, VOL. 48, NO. 11.

[7]. N.V. Grebennikov, A.V. Kireev and N.M. Kozhemyaka. (2015). Mathematical Model of Linear Switched Reluctance Motor with Mutual Inductance Consideration, International Journal of Power Electronics and Drive System (IJPEDS) , Vol. 6, No. 2, pp. 225~232.

[8]. B.H. Nguyen and C. M. Ta. (2011). Finite Element Analysis, Modeling and Torque Distribution Control for Switched Reluctance Motors with High Non-linear Inductance Characteristics, IEEE International Electric Machines & Drives Conference (IEMDC).

[9].J.F. Pan, Y. Zou and G.Cao. (2012). Adaptive controller for the double-sided linear switched reluctance motor based on the nonlinear inductance modelling, IET Electric Power Applications.

[10]. X. Li and P. Shamsi. (2015). Inductance Surface Learning for Model Predictive Current Control of Switched Reluctance Motors, IEEE Transactions On Transportation Electrification, VOL. 1, NO. 3.

[11]. R. Ajengui. (2004). Calculations approaches by finite elements of the thrust force of a tubular linear actuator, Automatic and signal treatment Master. National School Engineers of Tunis, Tunisia.

[12]. H. P. Chi. (2005). Simplified flux-linkage model for switched-reluctance motors, IEE Proc.Electr. Power Appl. 152(3).

[13]. Y. Kano, T. Kosaka, and N.Matsui. (2002). Magnetization characteristics analysis of SRM by simplified nonlinear magnetic analysis, Proc. Power Conversion Conf: 689–694.

[14]. K. N. Srinivas, and R. Arumugam. (2003). Dynamic characterization of switched reluctance motor by computer-aided design and electromagnetic transient simulation, IEEE Trans. Magn. 39(3):1806–1812.

[15]. D. Uday. (2000). Two-Dimensional Finite-Element Analysis of a High-Force-Density Linear Switched Reluctance Machine Including Three-Dimensional Effects, IEEE transactions on industry application. 36(4).

[16]. D. K. Hong, D. Joo, B. C. Woo and P. W. Han. (2014). The investigation on a thrust force 8,000 N class transverse flux linear motor, International Journal of Applied Electromagnetics and Mechanics, vol. 45, no. 1-4.

[17]. M. R. Zare, N. Misron, I. Aris and H. Wakiwaka. (2014). Analytical and experimental approach of the high density transverse flux linear stepper motor ," International Journal of Applied Electromagnetics and Mechanics, vol.46, no. 1.

[18]. J. Dai and S. Chang. (2014). Loss analysis of electromagnetic linear actuator ", International Journal of Applied Electromagnetics and Mechanics, vol. 46, no. 3.

[19]. D. Susitra and S. Paramasivam. (2014). Non-linear flux linkage modeling of switched reluctance machine using MVNLR and ANFIS, Journal of Intelligent & Fuzzy Systems, vol. 26, no. 2.

[20]. X. Jiang, J. Wang, Y. Li and J. Li. (2014). Design and modelling of a novel linear electromagnetic vibration energy harvester, International Journal of Applied Electromagnetics and Mechanics, vol. 46, no. 1.

[21]. M. Imed and R. Habib. (2016). Design and modeling of open-loop components for a biomedical application, Int. Trans. Electr. Energ. Syst, Published online in Wiley Online Library (wileyonlinelibrary.com),DOI: 10.1002/etep.2204.

[22]. M. Imed and R. Habib. (2016). Design, nonlinear modelling and performances of a biomedical system, International Journal of Applied Electromagnetics and Mechanics, vol. 50, no. 1, pp. 127-143.

[23]. M. Ali and S. Abbas. (2012). Inductance profile calculation of step winding structure in tubular linear reluctance motor using three dimensional finite element method, Euro. Trans. Electr. Power; 22:721–732.

[24]. J. Faiz and K. Moayed-zadeh. (2009). Design optimization of switched reluctance machines for starter/generator of hybrid electric vehicle by genetic algorithm , Euro. Trans. Electr. Power; 19:302–312.

[25]. M. Rekik, M. Besbes, C. Marchand, B. Multon, S. Loudot and D. Lhotellier. (2008). High-speed-range enhancement of switched reluctance motor with continuous mode for automotive applications, Euro. Trans. Electr. Power; 18:674–693

[26]. F. Jawad, B. Rezaeealam and P. Pillay. (2006). Adaptive performance improvement of switched reluctance motor with two-phase excitation, Euro. Trans. Electr. Power; 16:1–13.

Appendix

Table 1. Dimensional characteristics of the all biomedical system.

Dimensions of the used syringe		
volume of the syringe	V	*60 ml*
Piston mass	m_s	15 g
Length of the cylinder	L_c	118 *mm*
External diameter of the cylinder	D_c	30.11 *mm*
Internal diameter of the cylinder	D_e	27.48 *mm*
Tube length	L_t	1600 *mm*
Inner diameter of the tube	D_t	3.7 *mm*
Needle length	L_s	69.7 *mm*
Needle diameter	D_s	0.8 *mm*
Required thrust force	F	*4N*
Rated voltage	U	*14 V*
Rated current	I	*1 A*
Motor mechanical and electrical Parameters		
Number of modules	m	*4*
Tooth width	b	*3mm*
Slot width	a	*3mm*
Tooth pitch	λ	*6mm*
Phase separation	c	*1.5mm*
Mover length	L_m	*135 mm*
stator length	L_s	*40.5 mm*
Air gap width	δ	*0.1mm*
Height of the stator teeth	H_s	*17mm*
Height of the mover teeth	H_m	*4mm*
Depth of the actuator	D	*30mm*
Number of turns per phase		*520*

Table 3. Infusion Volume versus infusion time and the cycles number.

Number of power cycles	Infusion Volume (ml)	Infusion time (s)
1	1.5	4
2	3	8
3	4.5	12
4	6	16
….	….	…..
20	30	80

Table 2: coefficients of Eqs (9), (10), (11), (12), (13) and (14)

Coefficients of Eq (9)	Coefficients of Eq (10)	Coefficients of Eq (11)
a_6 = -0.14964	b_6 = -0.29455	c_6 = -0.10415
a_5 = 0.40276	b_5 = 1.0098	c_5 = 0.39906
a_4 = -0.34888	b_4 = -1.2404	c_4 = -0.54238
a_3 = 0.18654	b_3 = 0.68632	c_3 = 0.31762
a_2 = -0.17356	b_2 = -0.22522	c_2 = -0.1048
a_1 = 0.0085628	b_1 = 0.015891	c_1 = 0.0085593
a_0 = 0.15724	b_0 = 0.12801	c_0 = 0.099954
Coefficients of Eq (12)	**Coefficients of Eq (13)**	**Coefficients of Eq (14)**
d_6= 0.2779	e_6= -0.8095	h_6= 0.3820
d_5 = -1.0691	e_5 = 2.9400	h_5 = -1.4681
d_4 = 1.4731	e_4 = -3.8375	h_4 = 2.0155
d_3 = -0.7963	e_3 = 2.0967	h_3 = -1.1139
d_2 = 0.0685	e_2 = -0.4154	h_2 = 0.1733
d_1 = -0.0091	e_1 = 0.0354	h_1 = -0.0177
d_0 = 0.1300	e_0 = -0.0028	h_0 = 0.0301

Contribution of Individual Authors to the Creation of a Scientific Article (Ghostwriting Policy)

The authors equally contributed in the present research, at all stages from the formulation of the problem to the final findings and solution.

Sources of Funding for Research Presented in a Scientific Article or Scientific Article Itself

No funding was received for conducting this study.

Conflict of Interest

The authors have no conflicts of interest to declare that are relevant to the content of this article.